applied sciences

MDPI

Article

Evaluation of Low-Field NMR T_2 Methods for Residual Oil Saturation Estimation in Carbonate Core Plugs

Lamees Al-Siyabi [1,2], Lionel Esteban [2], Mustafa Sari [2], Ausama Giwelli [3] and Alireza Kazemi [1,*]

[1] Faculty of Petroleum Engineering, Department of Petroleum and Chemical Engineering, College of Engineering, Sultan Qaboos University, Muscat 123, Oman; s66853@student.squ.edu.om
[2] CSIRO Energy Research Unit, Perth 6151, Australia; mustafa.sari@csiro.au (M.S.)
[3] Inpex, Perth 6000, Australia
* Correspondence: a.kazemi@squ.edu.om

Abstract

Nuclear magnetic resonance (NMR) relaxometry is widely used to characterize pore systems and estimate fluid saturations in reservoir rocks. This study evaluates the use of low-field NMR transverse relaxation time (T_2) as a standalone method for estimating residual oil saturation in Indiana limestone core plugs following brine flooding. Three core plugs were first saturated with dead light crude oil and then subjected to brine core-flooding experiments at different injection rates to establish different post-flood residual oil saturations. Two NMR T_2-based approaches were investigated: (i) a volumetric method based on a calibrated T_2 cutoff and (ii) a mathematical method based on the logarithmic mean T_2 response. Independent saturation estimates were obtained using X-ray computed tomography (XCT). Overall, the volumetric approach showed closer agreement with XCT than the logarithmic mean approach. However, appropriate cutoff calibration and sensitivity analysis are essential because rock wettability, desaturation conditions, fluid properties, and pore-size distribution can influence cutoff selection and the resulting saturation estimates. At a T_2 cutoff of 90 ms, the cutoff-based oil saturation estimates were 42.0%, 38.8%, and 40.1% for Ind03, Ind08, and Ind09, respectively. Increasing the cutoff from 70 to 100 ms increased the estimated saturations by 4.4–5.0 percentage points across the three plugs, highlighting the sensitivity of quantitative saturation estimates to cutoff selection.

Keywords: residual oil; Indiana carbonate; nuclear magnetic resonance; X-ray CT (XCT); SCORES simulation

1. Introduction

The identification of water, oil, and gas in reservoir rocks typically begins with well logging. Combinations of resistivity, density, neutron, sonic, dielectric, and nuclear magnetic resonance (NMR) logs are used to estimate fluid saturations and distinguish oil, water, and gas in situ [1]. Resistivity-based methods exploit the strong conductivity contrast between saline water and hydrocarbons, while neutron–density cross-plots and dielectric measurements help resolve gas effects and fluid typing. Further, NMR logging provides estimates of movable versus bound fluids. However, these interpretations are inherently indirect and sensitive to rock texture, wettability, clay content, salinity, and tool responses. Therefore, laboratory calibration using representative core samples is essential to validate and constrain logging-derived estimates of fluid saturations and volumes.

Laboratory methods provide this ground truth through direct or physics-based measurements (Table 1). Classical techniques (see API Recommended Practice 40 for more

Check for updates

Academic Editor: Jan Vinogradov

Received: 19 August 2026
Revised: 16 October 2026
Accepted: 19 October 2026
Published: 29 October 2026

Copyright: © 2026 by the authors. Licensee MDPI, Basel, Switzerland. This article is an open access article distributed under the terms and conditions of the Creative Commons Attribution (CC BY) license.

details) such as Dean–Stark extraction, retort, and distillation can quantify oil and water contents by solvent extraction or thermal separation [2]. However, these methods are time-consuming and may alter rock properties. Thermogravimetric analysis (TGA) tracks fluid mass loss as temperature increases but requires independent measurements to confirm the interpretation. In comparison, imaging approaches like X-ray computed tomography (XCT) enable non-destructive visualization and quantification of fluid distributions at the pore scale. However, XCT can be time-consuming and costly, and its ability to resolve fluid distributions is limited by voxel size relative to pore size. Electrical resistivity measurements on cores are used to calibrate Archie-type relationships, although assumptions such as complete pore connectivity may not hold for all rocks. Chemical tracer and core-flooding experiments assess fluid saturations, displacement efficiencies, and wettability under dynamic conditions, but require specialized equipment and substantial experimental time.

Table 1. Summary of laboratory techniques to measure oil and water content in rock samples.

Category	Technique	Measures Oil/Water Separately	Destructive	Cost Effective
Direct extraction	Dean–Stark	Yes	Yes	No
Thermal	Retort	Limited	Yes	No
Electrical	Resistivity	Indirect	No	Yes
Dynamic	Core flooding	Indirect	No	No
Imaging	XCT/μXCT	Yes	No	No
Nuclear	NMR	Yes	No	Yes

Laboratory NMR relates relaxation times to pore sizes and fluid types, providing a practical link between core measurements and downhole NMR logs. It offers a relatively rapid, inexpensive, and non-destructive approach to fluid characterization. Together, these laboratory techniques underpin reliable log interpretation by anchoring petrophysical models to measured fluid contents and rock–fluid interactions when upscaling to the reservoir.

Nuclear magnetic resonance (NMR) is widely used for characterizing pore systems and estimating fluid saturations through detection of fluid-dependent relaxation signals [3–7]. In conventional pulsed NMR logging applications, paramagnetic additives such as $MnCl_2$ have been added to drilling muds to suppress the water signal and isolate the oil response [8–10]. As a result, residual oil saturation can be estimated from the distribution of NMR transverse relaxation time T_2 [5,11,12]. More recently, fluid distribution and saturation in porous media have also been investigated using two-dimensional NMR spectra, particularly combined T_1–T_2 analysis [13,14]. Other studies have explored residual oil saturation as a function of pore-body size, while Kuang proposed the use of a T_2 cutoff value, representing the threshold between immobile and movable fluids, to estimate fluid saturations based on the relationship among oil saturation, rock wettability, and the NMR T_2 distribution [12,15]. Zhang investigated the effects of permeability and heterogeneity on oil displacement during chemical flooding using NMR imaging, with applications to enhanced oil recovery (EOR) in conventional reservoirs [16]. NMR is also useful for characterizing fluids in unconventional reservoirs, including gas hydrate and shale reservoirs, and for geothermal applications [17–19].

X-ray computed tomography (XCT) is another effective technique for estimating liquid saturation in core plugs. The technique measures X-ray attenuation to generate three-dimensional images of the sample and has been widely applied in multiphase flow studies in porous rocks [20,21]. Previous studies demonstrated the effectiveness of XCT scanning for quantifying two-phase saturation after core-flooding experiments, and the method has also been extended to the estimation of three-phase saturations [22–24]. Despite its value

as an independent saturation measurement technique, XCT analysis can be experimentally demanding and costly, requires specialized image-processing expertise, and is often used to validate other methods.

Comparative evaluation of NMR-based methods for quantifying fluid saturations in carbonate rocks remains limited. This study evaluates two low-field NMR T_2 approaches, a cutoff-based volumetric method and a logarithmic mean method, for estimating residual oil saturation in Indiana limestone. Three core plugs were saturated with dead crude oil and subsequently flooded with brine at different injection rates. The NMR estimates were compared with independent XCT measurements. The study provides a proof of concept for the tested rock–fluid system and examines the sensitivity of saturation estimates to cutoff selection.

2. Methodology

2.1. Materials

Ten Indiana carbonate core plugs, each measuring 3.8 cm (1.5 in) in diameter and 5.08 cm (2 in) in length, were prepared from an Indiana carbonate block procured from Kocurek Industries (Caldwell, TX 77836, USA). Porosity and permeability were measured for the core plugs by nitrogen gas pycnometry (AP608 from Coretest Inc., Dover, Delaware) under an effective pressure of 250 psi, yielding average values of 14.7 ± 1% and 12 ± 2 mD, respectively. Three plugs were selected from the core plug collection for brine–oil core-flooding experiments, while a fourth plug was selected for detailed NMR calibration. According to X-ray diffraction (XRD) analysis, all plugs were composed of 98.9 wt% calcite and 1.1 wt% quartz.

A Siemens Somatom X-cite medical XCT scanner (Erlangen, Germany) was used to image the plugs in the dry, brine-saturated, oil-saturated, and post-flood desaturated states, as well as the pure oil and brine used during the saturation and desaturation procedures for calibration. The XCT scanner was operated at 140 kV and 500 mAs with helical acquisition using a pitch of 0.35 mm and a slice thickness of 0.5 mm. The acquired XCT images had a matrix size of 1024 × 1024 pixels and reached a voxel resolution of 50 × 50 × 100 µm using the smallest field of view and were reconstructed using the Siemens sharp kernel algorithm (Qr72) without AI-driven image correction or enhancement (Admire tool not active). XCT imaging confirmed that the selected plugs were homogeneous, with no distinct geological features or preparation-induced cracks.

The mean *CT* number of each *CT* slice was extracted to calculate the overall mean *CT* value and standard deviation of each sample. The mean *CT* values of the plugs at 100% brine saturation and 100% oil saturation (Table 2 and Figure 1) were then used to calibrate the *CT* response for estimating oil and brine saturations in the tested plugs after being brine core-flooded to residual oil saturation conditions, following the approach of Akin and Kovscek, and Alvestad [20,25]:

$$CT_x = (1 - ø)CT_{dry} + ø(S_w CT_w + S_{wo} CT_o) \quad (1)$$

$$S_o = \frac{CT_x - CT_{dry}}{CT_o - CT_{dry}} \quad (2)$$

where ø is porosity (fraction unit), CT_x is the mean *CT* value of the tested sample after core-flooding, CT_{dry} is the mean *CT* value in the dry state, and CT_w and CT_o are the mean *CT* values at 100% brine saturation and 100% oil saturation, respectively. S_w and S_o represent water saturation and oil saturation, respectively.

Table 2. XCT values used for calibration of oil–brine saturation estimates.

Sample State	CT (HU)
Air	-1000 ± 5
Pure water	0 ± 1
Brine	381 ± 1
Oil	-102 ± 2
Dry sample	2050 ± 5
Oil-saturated sample	2190 ± 5
Brine-saturated sample	2250 ± 5

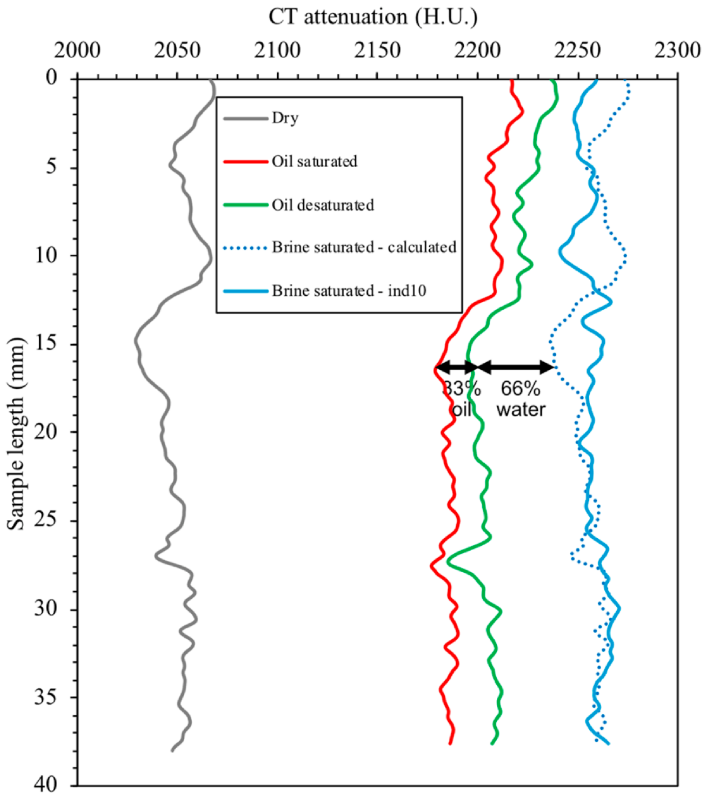


Figure 1. XCT profiles used for calibration of the *CT*-based saturation estimates.

Because the *CT* contrast between oil and brine was relatively small, despite iodide doping of the brine, accurate background correction and careful *CT* calibration were essential for reliable saturation estimation. It should be noted that the reported *CT* values are consistent with these observations [26].

The dry and oil-saturated profiles correspond to the Ind06 core plug (grey and red curves, respectively), whereas the brine-saturated profile was obtained from Ind10 (blue curve). For comparative visualization, the brine-saturated profile of Ind06 (dashed blue curve) was estimated using Equation (1). The green curve represents the post-flood XCT profile used to estimate the residual oil saturation of Ind06 using Equation (2).

For the experimental work, a light dead crude oil was used as the oil phase, with a density of 0.81 g/cm^3 and a viscosity of 2.7 cP, both measured at 377 °K and 55 MPa. The brine phase consisted of 3 wt% sodium chloride (NaCl) and 2 wt% potassium iodide (KI) dissolved in deionized water. Potassium iodide was added to enhance the contrast between the brine and oil phases in XCT imaging. This salinity level is representative of typical reservoir formations. In this study, the mean CT values were used to calculate oil and brine saturations before and after desaturation during brine core-flooding.

Pore-size distribution was measured by mercury intrusion capillary pressure (MICP) using a Micromeritics AutoPore IV 9500 from Micromeritics Instrument Corporation (Nor-

cross, GA, USA) on an offcut core plug from the Indiana carbonate block. Mercury pressure was applied from atmospheric pressure up to 420 MPa, enabling measurement of pore-throat radii as small as 3 nm. The Indiana carbonate exhibited a mean pore radius of ~0.3 µm, which is consistent with previously reported values [27,28].

2.2. Sample Preparation

The three plugs selected for the core-flooding experiments were first dried under vacuum at 105 °C for 48 h. The dried plugs were then placed in custom-built saturation cells under vacuum for 2 h. Crude oil was subsequently injected, and the hydrostatic pressure was increased to 10.3 MPa (1500 psi) at a rate of 0.7 MPa/min (100 psi/min) using a Teledyne ISCO pump from Teledyne ISCO (Lincoln, NE, USA). This pressure was maintained for 24 h to maximize oil saturation in the smallest pores (Figure 2).

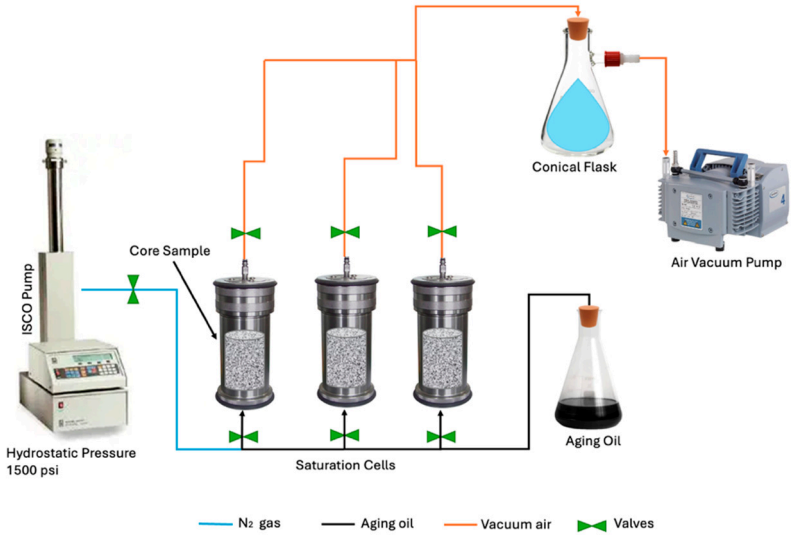


Figure 2. Schematic diagram of the setup used to saturate the Indiana limestone samples with oil.

After the 24 h saturation period, the hydrostatic pressure was gradually reduced at 0.7 MPa/min (100 psi/min). The plugs were immediately transferred to sealed glass vials containing the same crude oil and stored under ambient conditions. This ensured continued exposure of the samples to oil for two different aging periods (Table 3): (i) approximately 6 days and (ii) 83 days. A fourth core plug (Ind10) was saturated with brine using the same procedure described above and used for XCT and NMR data calibration.

Table 3. Petrophysical properties, sample masses, and initial and post-aging fluid saturations of the Indiana limestone plugs. † Porosity was determined by NMR for Ind08 and Ind09. ‡ Porosity was determined by water imbibition for Ind10. Nitrogen gas porosity measurements were unavailable for these plugs.

Sample	Length	Diameter	Porosity	Pore Volume	Permeability	Dry Sample Mass	Oil Saturated Sample Mass	Initial Oil Saturation	Oil Aging Duration	Water Saturated Sample Mass	Water Saturation
#	cm	cm	%	cm^3	mD	g	g	%	Days	g	%
Ind03	4.9	3.9	14.7	8.4	10.7	129.1	135.9	99.9	83	N/A	N/A
Ind08	5.1	3.9	† 15.7	9.5	N/A	132.9	140.6	99.9	7	N/A	N/A
Ind09	5.1	3.9	† 15.7	9.4	N/A	133.4	141	99.7	6	N/A	N/A
Ind10	5.56	3.84	‡ 15.2	9.8	N/A	146	N/A	N/A	N/A	155.8	99

The mass of each core plug was recorded in both dry and fully oil/water saturated states. The initial oil volume and saturation were then calculated using mass balance as described in Equations (3)–(7):

$$V_{Oil} = \frac{Mass_{oil\ saturated} - Mass_{dry}}{\rho_{oil}} \quad (3)$$

$$V_{water} = \frac{Mass_{water\ saturated} - Mass_{dry}}{\rho_{water}} \quad (4)$$

$$V_{Pore} = \emptyset \times V_{bulk} \quad (5)$$

$$S_{oil} = \frac{V_{oil}}{V_{pore}} \quad (6)$$

$$S_{water} = \frac{V_{water}}{V_{pore}} \quad (7)$$

where V_{oil} and V_{water} are the measured oil and water volumes in the saturated plugs, respectively; $Mass_{dry}$, $Mass_{oil\ saturated}$, and $Mass_{water\ saturated}$ are the sample masses in the dry, oil-saturated, and water-saturated states, respectively; V_{pore} is the pore volume of the sample; and ϕ is the porosity measured by gas pycnometry. S_{oil} and S_{water} represent oil and water saturation, respectively. The petrophysical properties of the selected core plugs and the initial saturation conditions are presented in Table 3.

2.3. Core-Flooding Experimental Setup and Workflow

Following oil aging, the core plugs were subjected to brine flooding to displace oil and establish residual oil saturation (S_{or}). Different brine injection rates were applied to establish a range of residual oil saturation conditions. The core-flooding system comprised a core holder connected to three pumps (Figure 3): (i) a hydraulic pump to maintain the confining pressure at 2500 psi, (ii) a Vindum pump to control the brine injection rate, and (iii) an ISCO pump to maintain the back pressure at 1500 psi. An in-house software package (Serendipity 1.1.0.111) controlled the injection and back-pressure pumps and recorded pressure, flow rate, and injected volume at 1 s intervals.

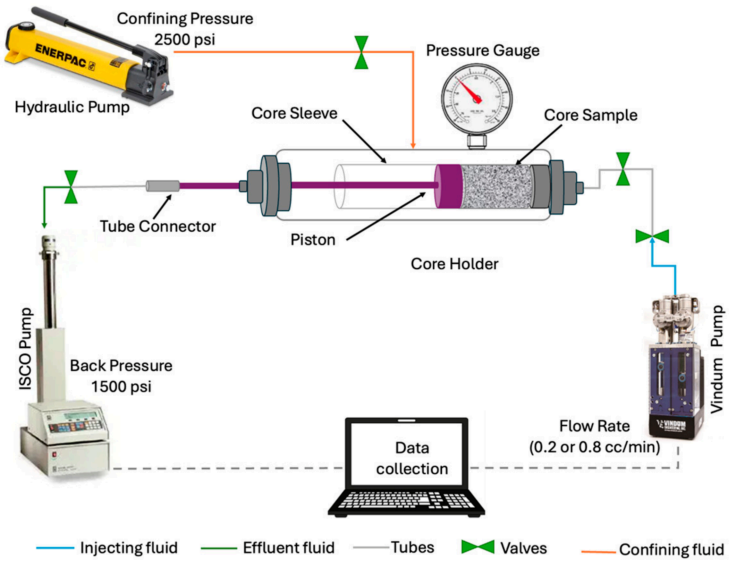


Figure 3. Schematic diagram of the brine core-flooding setup.

The experimental injection rates were selected using the SCORES core-flooding simulator [29,30]. The flooding process was modeled as an unsteady-state imbibition process

under progressively increasing water injection rates. The model assumed negligible entry capillary pressure, consistent with MICP data measured on Indiana samples and reported values below 1 psi for similar porous media, and homogeneous rock properties (as supported by the XCT observations) [31]. Relative permeability was not measured for the tested plugs. Therefore, endpoint values were obtained from a published study of Indiana limestone with a permeability of 7 mD and a porosity of 15%, using fluids with a brine density of 1.04 g/cm^3, an oil density of 0.73 g/cm^3, an oil viscosity of 0.89 cp, and an initial oil saturation of 91% [32]. Using these literature-derived values introduces uncertainty that may affect the accuracy of the simulations. The water injection rate was increased over a 7-day period, and oil saturation was calculated from the simulated oil displacement along the core length.

The SCORES simulations predicted an increase in water saturation with increasing injection rate. Higher flow rates promoted greater oil displacement and reduced the time required to reach stable saturation conditions. Two injection rates were selected for the brine-flooding experiments: 0.2 cm^3/min, corresponding to a predicted residual oil saturation of 40%, and 0.8 cm^3/min, corresponding to a predicted residual oil saturation of 23% (Supplementary Materials). These two conditions were selected to assess the effect of injection rate on imbibition displacement and the resulting residual oil saturation.

Each core plug was enclosed in a Viton sleeve and positioned between two stainless steel end platens equipped with fluid ports. The assembly was placed inside a core holder and secured. The confining chamber was filled with confining fluid while allowing air to escape through a dedicated port to prevent air entrapment. Confining pressure was then gradually increased to 2500 psi. Prior to injection, all pore lines and pumps were flushed with brine to remove residual air. Brine was subsequently injected at a constant rate of 0.2 cm^3/min for Ind03 and 0.8 cm^3/min for Ind08 and Ind09, up to a total injected volume of 10 pore volumes (PV) for each sample. During injection, pore pressure was increased to 1500 psi and maintained using the back-pressure pump.

Oil production was initially observed, followed by two-phase flow after breakthrough, and ultimately single-phase brine flow. Steady-state conditions were assumed once both pressure and flow rate stabilized at the injection and back-pressure pumps. These conditions were typically reached after the injection of approximately 10 pore volumes (PV) of brine. Because the experimental setup did not include an oil–brine separation system, produced oil volumes could not be quantified. Consequently, residual oil saturation could not be determined by material balance. At the end of each experiment, pore pressure was reduced to atmospheric pressure, followed by a controlled reduction in confining pressure at approximately 100 psi/min. The core samples were then weighed, sealed with cling film to minimize fluid loss, and stored horizontally at low temperature prior to NMR measurement to limit fluid redistribution.

2.4. NMR Methodology

2.4.1. NMR Relaxation in Porous Media

NMR measurements characterize the relaxation behavior of hydrogen nuclei within fluids occupying the pore space. The measured relaxation response is governed by three principal mechanisms: bulk fluid relaxation, surface relaxation, and diffusion relaxation [33,34]. The transverse relaxation time, T_2, can be expressed as follows [11,33,35–37]:

$$\frac{1}{T_2} = \frac{1}{T_{2bulk}} + \frac{1}{T_{2surface}} + \frac{1}{T_{2diffusion}} \quad (8)$$

Here, T_2 is the transverse relaxation time, T_{2bulk} is the bulk-fluid relaxation time; $T_{2surface}$ is the surface relaxation time associated with fluid–solid interactions; and $T_{2diffusion}$

is the relaxation time associated with molecular diffusion in the presence of a magnetic field gradient.

$$\frac{1}{T_{2bulk}} = C\left(\frac{298\eta}{T_k}\right) \tag{9}$$

where T_k is the temperature in kelvin, C is a proportionality constant in the bulk relaxation term, and η is the fluid viscosity.

$$\frac{1}{T_{2surface}} = \rho\left(\frac{S}{V}\right) \tag{10}$$

Here ρ is the surface relaxivity, and $\frac{S}{V}$ is the pore surface-area-to-volume ratio.

$$\frac{1}{T_{2diffusion}} = \frac{D(\gamma G T_e)^2}{12} \tag{11}$$

where $(\frac{1}{T_{2diffusion}})$ is the diffusion-induced relaxation rate of a fluid confined within the pore space. D is the confined fluid diffusion coefficient (gas, oil, or water), γ is the gyromagnetic ratio of a proton (2.675×10^8 s^{-1} T^{-1} for ^1H nuclei), G is the internal magnetic field gradient (G/cm), and T_e is the total echo time between the initial pulse and the peak of the detected echo signal (ms) [38].

The wettability of core plugs can also be evaluated using the NMR wettability index proposed by Fleury [39]. This index is determined from measurements of fully water-saturated and fully oil-saturated samples, followed by centrifugation to obtain the lowest achievable water and oil saturations, respectively [39]:

$$C_\rho = \frac{1/T_{w100} - 1/T_{bw}}{1/T_{o100} - 1/T_{bo}} \tag{12}$$

where C_ρ is the water–oil surface relaxivity ratio, and T_{w100} and T_{o100} are dominant relaxation times in the NMR T_2 distribution for water and oil at 100% saturation, respectively. T_{bw} and T_{bo} are the bulk relaxation times for water and oil, respectively.

$$I_{NMR} = \frac{S_w(1/T_w - 1/T_{bw}) - C_\rho S_o(1/T_o - 1/T_{bo})}{S_w(1/T_w - 1/T_{bw}) + C_\rho S_o(1/T_o - 1/T_{bo})} \tag{13}$$

Here, I_{NMR} is the NMR wettability index; T_w is the dominant relaxation time at the lowest achievable water saturation (S_w); and T_o is the dominant relaxation time at the lowest achievable oil saturation (S_o).

A GeoSpec II-53 NMR instrument from Oxford Instruments Ltd. (High Wycombe, UK). was used to record T_2 distributions for all Indiana limestone core plugs after the core-flooding experiments. The acquisition parameters are listed in Table 4.

Table 4. NMR acquisition parameters used in this study.

NMR Parameter	Setting
NMR frequency (MHz)	2.33
Echo spacing (T_e) (μs)	130
Repetition time (T_r) (ms)	7500

2.4.2. NMR Procedure

Residual oil saturation was estimated in this study using NMR transverse relaxation time (T_2). In previous studies, NMR T_2 has often been combined either with NMR T_1, which increases acquisition complexity, time, and cost for well or reservoir characterization,

or with micro-XCT, which makes the workflow more labor-intensive and computationally demanding [13,14]. In contrast, this study aimed to develop a simplified approach based solely on NMR T_2, supported by appropriate calibration and interpretation. Two T_2-based methods were evaluated: (i) volumetric estimation and (ii) mathematical estimation.

Considerable effort was initially devoted to calibrating the NMR fluid volumes to ensure accurate quantification, as well as to converting the NMR T_2 distribution into an absolute pore size distribution, particularly for samples containing mixed brine and oil phases. For this purpose, a core plug (Ind10) with porosity and permeability comparable to those of the oil–brine core-flooded samples was selected (Table 3).

The Ind10 plug was fully saturated with brine using the experimental procedure described in Figure 2. Full brine saturation was verified by mass balance, using the pore volume previously determined from gas pycnometry. The NMR T_2 distribution of the fully brine-saturated Ind10 sample was then measured and compared with the pore size distribution obtained from mercury intrusion capillary pressure (MICP) analysis (Figure 4). The conversion from T_2 relaxation time to pore size was performed according to Coates [11]:

$$D = 2\rho T_2 \tag{14}$$

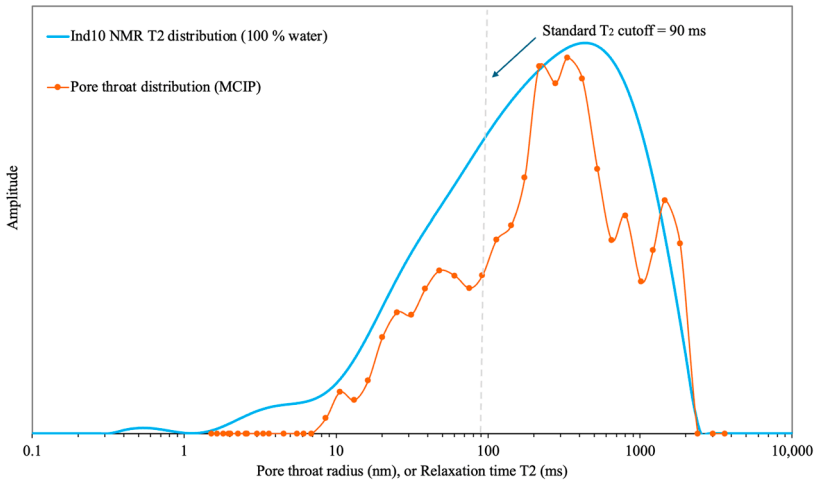


Figure 4. Pore-size distribution of the Indiana limestone sample. The orange curve represents the pore-throat size distribution obtained from MICP, whereas the blue curve represents the NMR T_2 distribution of the fully water-saturated Ind10 core plug.

Here, D is the pore diameter (in nm); ρ is the surface relaxivity; and T_2 is the transverse relaxation time (ms).

The first method relied on the determination of a T_2 cutoff value that separates smaller pores containing irreducible fluids from larger pores containing mobile or recoverable fluids [11,34,40]. In clastic rocks, irreducible fluids are generally assumed to consist predominantly of water, since these rocks are initially water-wet before oil migration. In carbonate rocks, prolonged exposure to oil can shift wettability toward mixed-wet or oil-wet conditions through interactions between polar oil components and calcite or dolomite surfaces. The Indiana limestone samples used in this study were obtained from a quarry and had not previously been exposed to oil. They were therefore expected to be water-wet before oil aging. Ind08 and Ind09 were assumed to remain predominantly water-wet because of their short aging periods, whereas Ind03 may have undergone wettability alteration during its 83-day aging period.

The T_2 cutoff value was determined on the Ind10 core plug using a centrifuge-based desaturation method [33,41]. The sample was first fully saturated with brine and measured by NMR. It was then desaturated in a Vinci Technologies centrifuge (model 4500) (Nanterre,

France) operated at 3500 rpm and 25 °C, corresponding to an applied capillary pressure of approximately 200 psi for this sample. Centrifugation was continued until no further brine production was observed in the transparent receiver canister. The sample was then immediately weighed and remeasured by NMR (Figure 5).

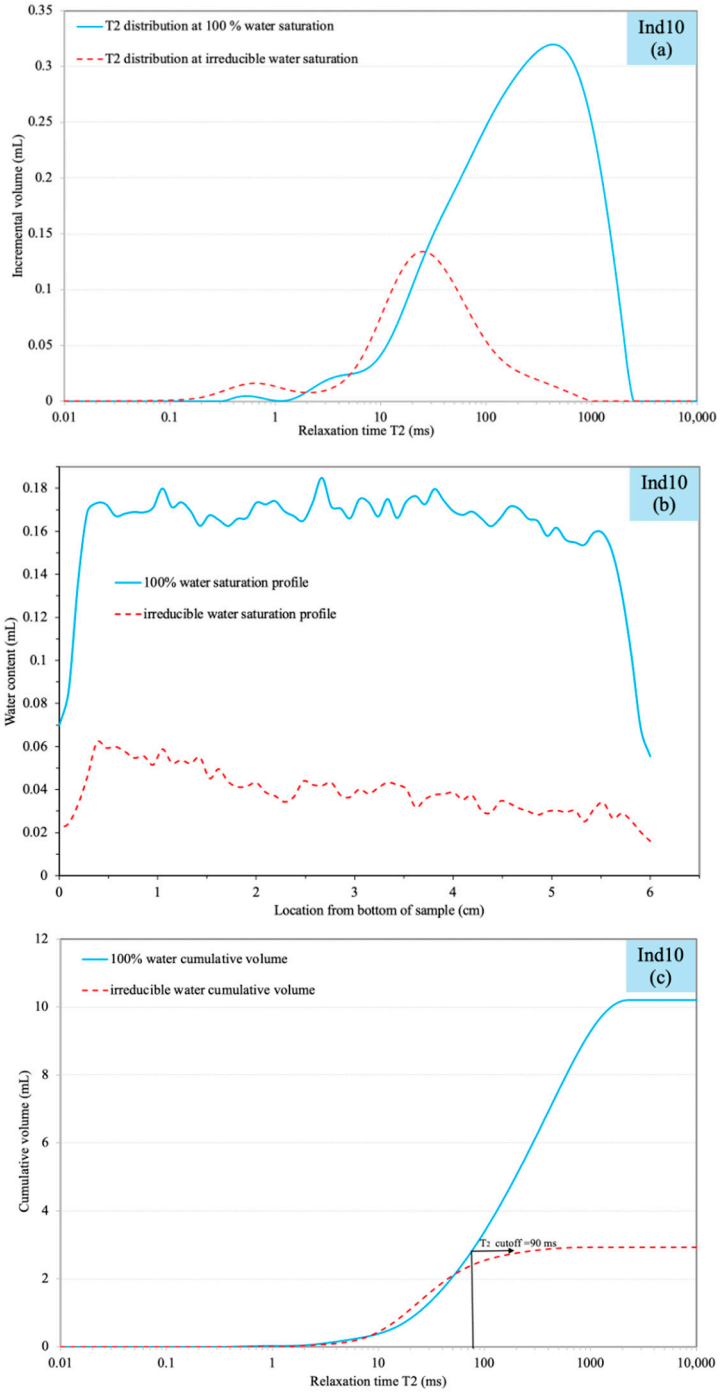


Figure 5. NMR measurements of Ind10 at full water saturation (blue curves) and after centrifugation to irreducible water saturation (red curves): (**a**) T_2 distributions; (**b**) water-content profiles; and (**c**) cumulative water-content curves used to determine the approximately 90 ms T_2 cutoff separating movable and irreducible water.

The NMR T_2 distribution of the fully brine-saturated Ind10 plug (Figure 5a) shows two pore-size populations: (i) larger pores at T_2 > 100 ms and (ii) smaller pores at T_2 < 100 ms, with a loss of water only from the large pores after desaturation by centrifugation. In

addition, the pore-throat size distribution obtained from mercury intrusion capillary pressure (MICP) analysis showed a similar pore-system partitioning (Figure 4), supporting the pore-size interpretation derived from NMR [42]. The combined use of MICP and NMR T_2 enabled conversion of relaxation time into an approximate pore-size distribution, with larger pores centered around ~0.3 μm and smaller pores below 0.01 μm.

At full water saturation, the NMR water-content profile was approximately flat, indicating a uniform distribution of water along the sample. After centrifugation, a slight gradient developed, with more water retained toward the bottom of the sample (Figure 5b). Comparison of the profiles before and after centrifugation indicated a water-content reduction of approximately 75%. The cumulative NMR T_2 curves for the fully saturated and desaturated states were compared (Figure 5c) to determine the T_2 cutoff value [11,40]. It should be noted that the T_2 cutoff may vary with centrifuge speed, applied capillary pressure, and the pore-body-to-pore-throat radius ratio [33,43]. However, standard practice is to centrifuge to reach a capillary pressure between 100 and 200 psi as applied to the Ind10 sample. The sample lost approximately 76% of its initial water content during centrifugation (i.e., irreducible water saturation is 24% assuming a brine density of 1.03 g/cm^3), consistent with the NMR T_2 distributions and water-content profiles obtained before and after centrifugation, demonstrating the high sensitivity and reliability of NMR for quantifying brine saturation changes. The cumulative water content of both saturated and desaturated curves led to a T_2 cutoff of ~90 ms, corresponding to a pore size of about 0.05 μm based on the MICP interpretation (Figure 4). A generalized T_2 cutoff value of approximately 90 ms is often reported for carbonate rocks to distinguish smaller from larger pores [40,44]. However, this threshold can slightly vary and should be calibrated for the specific rock type under investigation.

The centrifugation procedure was repeated for Ind08 using conditions similar to those applied to Ind10. The purpose was to determine the NMR wettability index using measurements from the fully water-saturated Ind10 plug and the fully oil-saturated Ind08 plug. After core flooding, Ind08 was cleaned and dried at 65 °C for one week to remove residual oil and water. It was then saturated with oil and aged using the procedure described for the core-flooding experiments. Finally, Ind08 was centrifuged at 3500 rpm and 25 °C under a capillary pressure of 200 psi until no further oil production was observed. The NMR T_2 profile was then recorded. The sample mass after centrifugation was 137.4 g, and the estimated oil saturation was 72%. Fluid saturations after centrifugation were calculated using the measured mass losses, fluid densities, and pore volumes (Table 5).

Table 5. Water and oil saturations after centrifugation.

Sample	Mass at 100% Saturation (Gram)	Mass After Centrifugation (Gram)	Fluid Type	Fluid Density (g/cc)	Pore Volume (cc)	Saturation After Centrifugation (%)
Ind 10	155.8	148.6	water	1.03	9.8	24.2
Ind 08	140.6	137.4	oil	0.81	9.5	72.4

The second method for estimating residual oil saturation was based on the logarithmic mean T_2 value (T_{2lm}). The logarithmic mean provides a distribution-weighted average relaxation time and is commonly used to characterize fluid occupancy in porous media [6,34,45,46]. In this study, (T_{2lm}) was used to quantify the shift in T_2 response between oil-saturated and brine-saturated states and thereby estimate the oil-to-water ratio after oil displacement during the core-flooding experiments. This approach requires the calculation of (T_{2lm}) for three conditions: (i) 100% oil saturation, (ii) 100% water saturation, and (iii) the desaturated state after flooding. The fully oil-saturated and fully water-saturated states

define the two end-member responses, while the intermediate desaturated state is used to estimate the relative proportions of oil and water. The logarithmic mean T_2 is defined in Equation (15) below [46]:

$$T_{2lm} = 10^{\left[\frac{\sum_{i=1}^{n} V_i \log(T_{2i})}{\sum_{i=1}^{n} V_i}\right]} \quad (15)$$

where V_i is the pore volume contribution, or incremental porosity, associated with a given relaxation time T_{2i}.

The oil percentage was estimated in the desaturated state from Equation (16). The equation is based on an end-member interpolation approach. The logarithmic mean relaxation time of the desaturated sample is assumed to lie between the responses of the fully oil-saturated and fully water-saturated states.

Under this assumption, the normalized shift can be used as a proxy for the relative fraction of oil remaining in the pore space. This approach is empirical and assumes approximately monotonic behavior with fluid saturation. Potential departures from this assumption may arise from the wettability effect, pore-size-dependent fluid distributions, surface relaxation heterogeneity, and nonuniform displacement of oil during flooding.

$$Oil(\%) = \frac{(T_{2lm})_{oil\ desat}}{(T_{2lm})_{100\%\ water} - (T_{2lm})_{100\%\ oil}} \quad (16)$$

After determining the T_{2lm} values for the fully oil-saturated, fully water-saturated, and post-flood desaturated states, oil saturation was calculated using Equation (16).

3. Results and Discussion

3.1. Calibration of NMR Oil and Brine Responses

The NMR instrument was calibrated using known volumes of brine–oil mixtures prepared from the same fluids used in the core-flooding experiments. The primary objective was to identify the respective oil and brine responses in the T_2 distribution and to verify that the signals from the two fluids were sufficiently separated to enable reliable deconvolution. Any significant overlap between the oil and brine signals would impede accurate phase discrimination and quantification. To assess this, NMR measurements were performed on mixtures prepared at different brine-to-oil volumetric ratios in glass vials, each with a total volume of 5 cm^3, as summarized in Table 6.

Table 6. Oil and water mixture samples.

Sample No.	Vial 1		Vial 2		Vial 3		Vial 4	
Fluid	Oil	Brine	Oil	Brine	Oil	Brine	Oil	Brine
Volume (cm^3)	4	1	3	2	2	3	1	4
Percentage (%)	80	20	60	40	40	60	20	80

The measured T_2 distributions indicate that the oil signal is located at approximately T_2 = 90 ms, whereas the brine signal is located at approximately T_2 = 3000 ms (Figure 6). This clear separation between the oil and brine T_2 responses provides the basis for distinguishing and quantifying the respective fluid phases within the core plugs. Given that the tested Indiana samples exhibit broadly similar porosity, permeability, pore structure, and mineralogy, the T_2 distributions of the partially saturated samples are expected to show the oil signal at shorter relaxation times and the brine signal at longer relaxation times, with sufficiently distinct populations to enable phase discrimination.

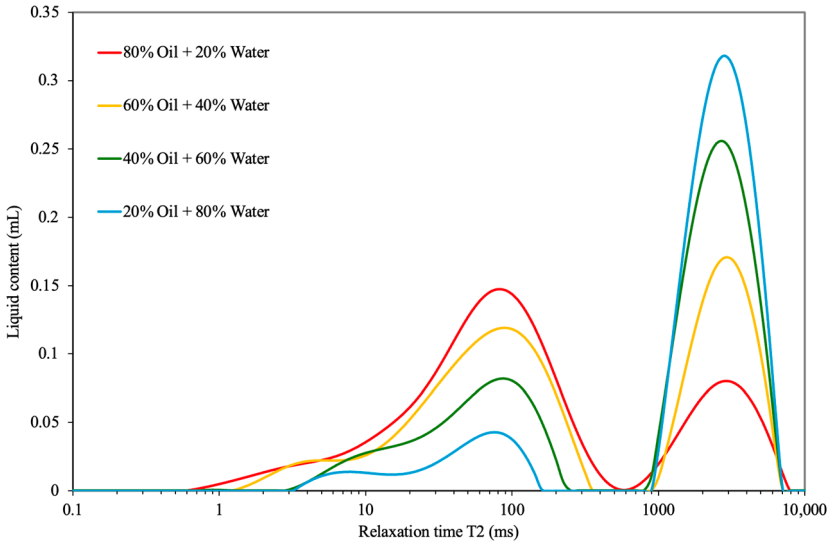


Figure 6. NMR T_2 distributions of oil–brine mixtures at different volumetric ratios in 5 cm^3 glass vials.

When the same method was applied to the Indiana limestone samples, Ind10 (fully brine-saturated) and Ind08 (fully oil-saturated) exhibited similar overall T_2 distribution patterns, reflecting their comparable pore structures (Figure 7). However, the distribution of the oil-saturated plug is shifted towards shorter T_2 values, whereas that of the fully brine-saturated plug is shifted towards longer T_2 values, consistent with the fluid-specific relaxation behavior observed previously (Figure 6). This trend is also evident in the partially desaturated state of Ind08 after brine core flooding (Figure 7; green curve), where the T_2 distribution shifts towards longer relaxation times as brine progressively displaces oil within the pore space.

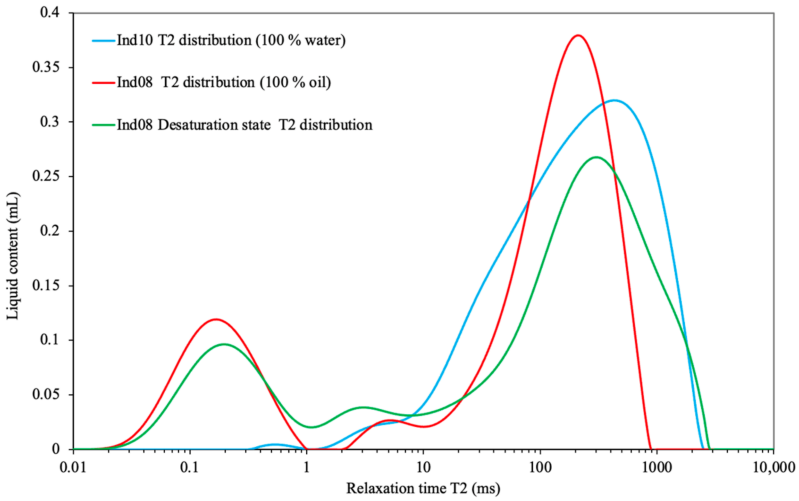


Figure 7. NMR T_2 distributions of Ind10 at full water saturation (blue), Ind08 at full oil saturation (red), and Ind08 after brine core flooding to residual oil saturation (green).

3.2. NMR Wettability Analysis

The wettability of Ind08 was evaluated using the NMR wettability index. The peak relaxation times required to calculate the surface relaxivity ratio were obtained from Figures 6 and 7. The dominant relaxation times after centrifugation, Tw and To, corresponding to the lowest measured water saturation (Sw = 24%) and oil saturation (So = 72%), respectively, were obtained from Figure 8.

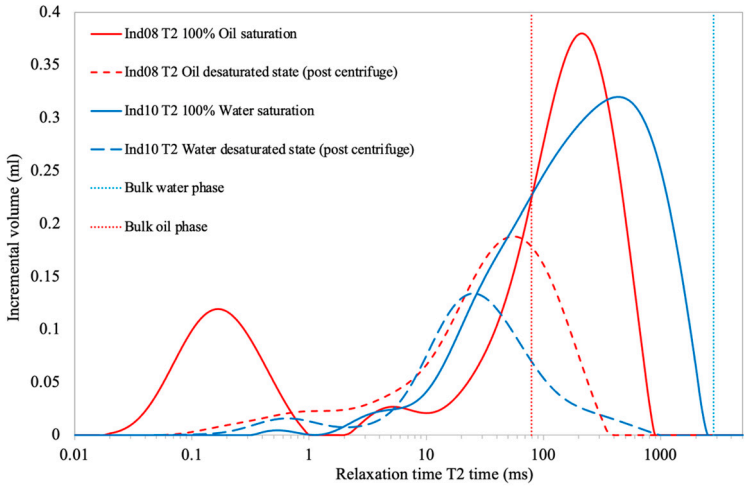


Figure 8. NMR T_2 distributions of Ind10 and Ind08. The solid and dashed blue curves represent Ind10 before and after brine desaturation by centrifugation, respectively. The solid and dashed red curves represent Ind08 before and after oil desaturation by centrifugation, respectively. The vertical dotted blue and red lines indicate the bulk brine and oil relaxation times.

The relaxation times and saturation values were substituted into Equations (12) and (13) to calculate the NMR wettability index. The resulting value, I_{NMR} = 1, indicated a water-wet tendency for Ind08 after seven days of oil aging.

3.3. Estimation of Residual Oil Saturation

3.3.1. Volumetric Estimation Using NMR T_2 Cutoff

The NMR T_2 distributions measured after brine flooding of the Indiana limestone plugs (Ind03, Ind08, and Ind09) show broadly similar behavior (Figure 9). Using the calibrated $T_{2cutoff}$ at 90 ms, the fluid signal at $T_2 > T_{2cutoff}$ was assigned predominantly to brine occupying the larger pores, whereas the signal at $T_2 < T_{2cutoff}$ was assigned predominantly to oil and irreducible fluids in the smaller pores. The fluid volumes estimated from T_2 distributions were corrected using Equations (17)–(20):

$$oil_{NMR}\ (\%) = \frac{\sum_{i=0}^{T2\ cutoff} V_{(i)_{NMR}}}{V_{(total)_{NMR}}} \quad (17)$$

$$water\ _{NMR}\ (\%) = \frac{\sum_{T_2\ cutoff}^{n} V_{(i)_{NMR}}}{V_{(total)_{NMR}}} \quad (18)$$

$$V_{oil} = V_{pore} \times oil_{NMR}\ (\%) \quad (19)$$

$$V_{water} = V_{pore} \times water\ _{NMR}\ (\%) \quad (20)$$

where $V_{(i)NMR}$ is the incremental volume associated with the ith T_2 bin; $V_{(total)_{NMR}}$ is the sum of all incremental volumes from NMR T_2 distributions; and V_{oil} and V_{water} are oil and water volumes after correction. $Water\ _{NMR}$ (%) and oil_{NMR} (%) are percentages of water and oil, respectively, estimated from the T_2 distributions. V_{Pore} is the core plug pore volume.

Accordingly, oil and brine saturations were estimated using Equations (6) and (7) for each core plug. The estimated residual oil saturations (at $T_{2cutoff}$ = 90 ms) were: (i) 42% for Ind03, (ii) 38.8% for Ind08, and (iii) 40% for Ind09. These results are physically consistent with the flooding conditions, as the lower brine injection-rate case (Ind03: 0.2 cm^3/min) retained slightly more oil than the higher brine injection-rate cases (Ind08 and Ind09: 0.8 cm^3/min). This trend is consistent with XCT, which indicated greater oil displacement and higher water saturation at higher injection rates.

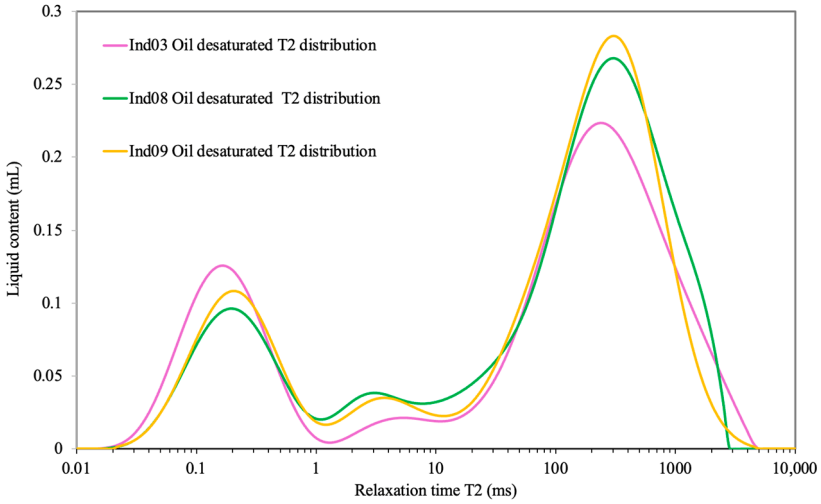


Figure 9. NMR T_2 distributions of the desaturated Indiana limestone plugs after brine core flooding. The purple, green, and yellow curves correspond to the residual oil states of Ind03, Ind08, and Ind09, respectively.

Ind08 and Ind09 were aged in oil for approximately one week, whereas Ind03 was aged for 83 days. The NMR wettability index indicated a water-wet tendency for Ind08. Ind09 was also expected to remain predominantly water-wet because of its similar aging period. The wettability index was not determined directly for Ind03; its possible alteration toward mixed-wet or oil-wet conditions is an assumption based on the longer aging period. Its higher estimated residual oil saturation may therefore reflect both the lower injection rate and possible wettability alteration.

3.3.2. Mathematical Estimation Using NMR T_2 Logarithmic Mean

The second approach estimated oil and water contents from the logarithmic mean T_2, using fully oil-saturated Ind08 (T_{2lm} = 32 ms) and fully water-saturated Ind10 (T_{2lm} = 179 ms) as calibration end members. The T_{2lm} values of the desaturated samples were 32.9 ms for Ind03, 49.0 ms for Ind08, and 40.8 ms for Ind09. These values were used to estimate the oil-to-water ratio and, subsequently, the residual oil saturation.

The calculated residual oil saturations from the logarithmic mean approach were 22.4% for Ind03, 33.0% for Ind08, and 27.7% for Ind09. Although the estimate for Ind08 is close to that obtained from the volumetric approach, the values for Ind03 and Ind09 are substantially lower. In addition, the expected relationship between injection rate and residual oil saturation is not clearly preserved.

3.4. NMR Approaches and Verification

XCT profiles acquired for the dry, fully oil-saturated, and oil-desaturated states were used to compute the residual oil saturation using Equation (2), and the results are summarized in Table 7. Figure 10 shows the XCT profiles for the dry (grey), fully oil-saturated (red), and post-flood desaturated (green) states. Differences between the profiles reflect changes in fluid content during brine flooding. Within each sample, the profiles are approximately parallel, suggesting a relatively uniform fluid distribution along the core. An exception occurs in Ind09 between 25 and 35 mm, where oil displacement was limited. This interval has lower CT values, interpreted as lower porosity, which may have restricted fluid flow relative to the rest of the sample. This difference is similar for Ind08 and Ind09, but larger for Ind03, indicating a higher degree of oil displacement in that sample.

Table 7. Mean XCT values for Ind03, Ind08, and Ind09 in the dry, fully oil-saturated, and post-flood desaturated states, together with the estimated residual oil saturations. The NMR volumetric estimates summarize sensitivity to the tested T_2 cutoffs.

Sample	Dry XCT (HU)	Oil Saturated XCT (HU)	Oil Desaturated XCT (HU)	So Desaturated from XCT (%)	So Desaturated from NMR Volumetric Method (%)
Ind03	2051 ± 9	2186 ± 19	2210 ± 15	38 ± 5	41 ± 3
Ind08	2051 ± 9	2186 ± 9	2206 ± 8	32 ± 3	38 ± 2
Ind09	2067 ± 10	2202 ± 10	2217 ± 11	33 ± 4	39 ± 3

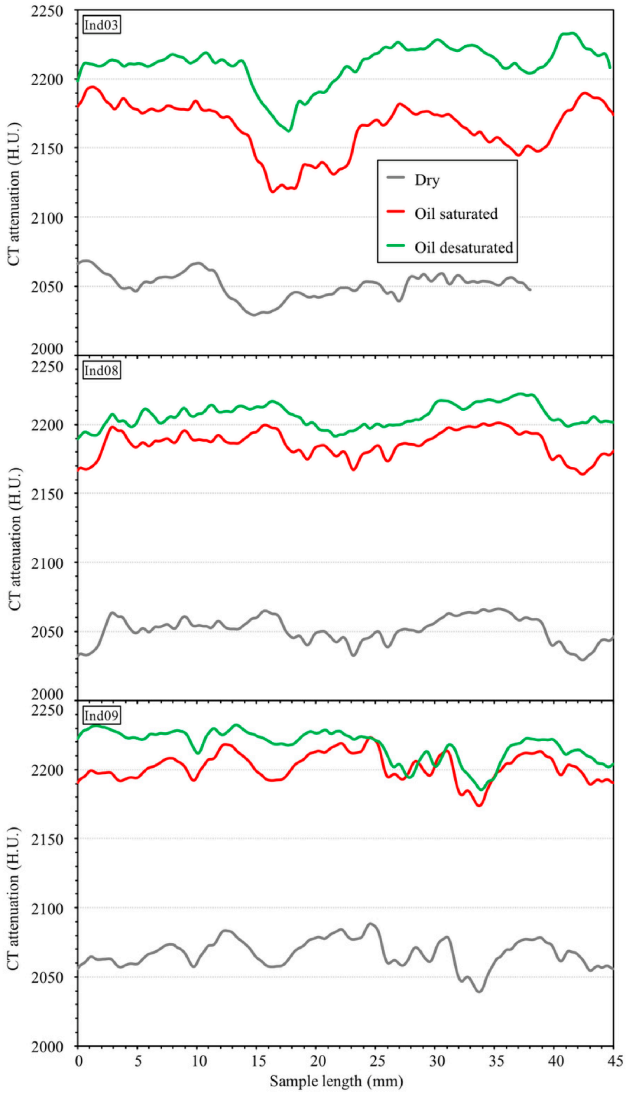


Figure 10. XCT profiles along the length of the three tested core plugs (Ind03, Ind08, and Ind09) in three states: (i) dry (grey), (ii) oil-saturated (red), and (iii) post-flood desaturated (green). The difference between the oil-saturated and desaturated profiles reflects the amount of oil displaced by brine, which is greater in Ind03 and lower but similar in Ind08 and Ind09.

Residual oil saturation estimates from the NMR volumetric approach were initially based on the cutoff calibrated using Ind10. However, differences in aging duration, wettability, and desaturation conditions may affect the appropriate cutoff for each plug. A sensitivity analysis was therefore conducted using cutoffs of 70, 80, 90, and 100 ms. The

mean saturation estimates and standard deviations across the tested cutoffs are summarized in Table 7. Estimates for the individual cutoffs are presented in Table 8, and their agreement with XCT is assessed in Table 9.

Table 8. Residual oil saturation estimates for Ind03, Ind08, and Ind09 obtained using XCT, the NMR volumetric method at different T_2 cutoffs, and the NMR logarithmic mean method.

Sample	So (XCT) (%)	So ($T_{2cutoff}$ = 70 ms) (%)	So ($T_{2cutoff}$ = 80 ms) (%)	So ($T_{2cutoff}$ = 90 ms) (%)	So ($T_{2cutoff}$ = 100 ms) (%)	So (Logarithmic Method) (%)
Ind03	38	38.9	40.4	42.0	43.9	22.4
Ind08	32	36.0	37.3	38.8	40.4	33.0
Ind09	33	37.0	38.5	40.1	41.9	27.7

Table 9. Summary of Mean Absolute Error (MAE), Root Mean Square Error (RMSE), and Mean Relative Error (MRE) for evaluating NMR-based approaches against XCT as a reference method.

Error Estimates	NMR T_2 ($T_{2cutoff}$ = 70 ms)	NMR T_2 ($T_{2cutoff}$ = 80 ms)	NMR T_2 ($T_{2cutoff}$ = 90 ms)	NMR T_2 ($T_{2cutoff}$ = 100 ms)	NMR T_2 (Logarithmic Method)
MAE	3.0	4.4	6.0	7.7	7.3
RMSE	3.3	4.6	6.1	7.8	9.5
MRE (%)	9%	13%	18%	23%	20%

The sensitivity analysis shows closer agreement with XCT at cutoffs below the calibrated value of 90 ms. Cutoffs of 70 and 80 ms yielded MRE values of 9% and 13%, respectively, compared with 18% and 23% at 90 and 100 ms. The preference for a lower cutoff may reflect the shorter T_2 response associated with oil in the flooded plugs, compared with the brine-only calibration sample, Ind10 (Figures 6 and 7). Among the tested values, 70 ms provided the closest agreement with XCT for this dataset. The logarithmic mean approach yielded an MRE of 20%. These results favor the volumetric approach with a lower cutoff under the investigated conditions.

Table 10 presents the contribution of the reported 0.1% porosity uncertainty of the CoreTest AP-608 porosimeter to the estimated oil saturation at cutoffs of 70, 80, 90, and 100 ms. Uncertainties associated with oil density, NMR calibration, and XCT calibration were not quantified independently. Therefore, the values in Table 10 do not represent the total uncertainty of the saturation estimates.

Table 10. Summary of porosity uncertainty propagated to the calculated oil saturation for each NMR T_2 cutoff value.

Sample	So ($T_{2cutoff}$ = 70 ms) (%)	So ($T_{2cutoff}$ = 80 ms) (%)	So ($T_{2cutoff}$ = 90 ms) (%)	So ($T_{2cutoff}$ = 100 ms) (%)
Ind03	0.26	0.27	0.28	0.29
Ind08	0.25	0.26	0.27	0.28
Ind09	0.25	0.26	0.27	0.28

4. Conclusions

This study evaluated the use of low-field NMR transverse relaxation time T_2 as a standalone method for estimating residual oil saturation in carbonate core plugs following brine flooding. Two NMR-based workflows were examined: (i) a volumetric approach

based on a calibrated $T_{2cutoff}$ and (ii) a mathematical approach based on the logarithmic mean T_2 response. XCT was also used to estimate residual oil saturation and provide a reference for comparison with the NMR approaches. The volumetric NMR approach showed promise under the investigated conditions. However, the appropriate T_2 cutoff depends on pore structure, wettability, mineralogy, fluid properties, and desaturation conditions. Although the three tested plugs originated from a single Indiana carbonate block and had similar pore-size distributions and mineralogy, applying one calibrated cutoff to all plugs may be inappropriate when injection rates and wettability differ.

These findings suggest that, with appropriate calibration, NMR T_2 measurements can provide a practical approach to fluid saturation estimation. The applicability discussed here is limited to homogeneous Indiana limestone containing light crude oil with a density below 0.9 g/cm^3 and sufficiently separated oil and water NMR signals. The results may not apply to heavy or viscous oils, mixed-wet systems, or heterogeneous carbonate reservoirs. Further experiments are needed to investigate the effects of fluid properties, fluid composition, and rock heterogeneity.

Under the investigated conditions, the cutoff-based volumetric approach performed better than the logarithmic mean method. The findings provide a proof of concept for NMR-based saturation estimation in the tested Indiana limestone and light-oil–brine system. Application to other carbonate lithologies and reservoir conditions requires further validation and rock-specific calibration of the T_2 cutoff.

Supplementary Materials: The following supporting information can be downloaded at: https://www.mdpi.com/article/10.3390/app162110710/s1.

Author Contributions: L.A.-S.: conceptualization, formal analysis, investigation, methodology, validation, data curation, writing—original draft. A.K.: supervision, conceptualization, project administration, formal analysis, validation, writing—review. L.E.: conceptualization, supervision, validation, methodology, writing—review and editing. M.S.: methodology, writing—review and editing. A.G.: conceptualization, writing—review and editing. All authors have read and agreed to the published version of the manuscript.

Funding: This research received no external funding.

Data Availability Statement: The original contributions presented in this study are included in the article. Further inquiries can be directed to the corresponding author.

Acknowledgments: All experiments were conducted at the Commonwealth Scientific and Industrial Research Organisation (CSIRO) in Perth, Australia. We thank the CSIRO Energy Resources Program for its financial and technical support and the technicians of the Geophysical and Geomechanical Laboratory for preparing the samples used in this study.

Conflicts of Interest: The authors declare no conflicts of interest.

References

1. Serra, O. *Well Logging Handbook*; Editions Ophrys: Paris, France, 2008.
2. RP40, A. Recommended Practices for Core Analysis. 1998. Available online: https://energistics.org/sites/default/files/2022-10/rp40.pdf (accessed on 24 May 2026).
3. Loren, J.D.; Robinson, J. Relations between pore size fluid and matrix properties, and NML measurements. *Soc. Pet. Eng. J.* **1970**, *10*, 268–278. [CrossRef]
4. Robinson, J.; Vajnar, E.; Loren, J.; Hartman, D. *Determination of Residual oil Using the Nuclear Magnetism Log*; Office of Scientific and Technical Information: Oak Ridge, TN, USA, 1971.
5. Setser, G.; Williams, M.R. Measurement of Remaining Oil Saturation in Northern Michigan Using Nuclear Magnetism Log Data and Pressure Core. In *SPE Annual Technical Conference and Exhibition*; SPE: Las Vegas, NV, USA, 1985.

6. Straley, C. Investigations of the Structure of Porous Media. Ph.D. Thesis, University of Delaware, Newark, DE, USA, 1995. Available online: https://www.proquest.com/dissertations-theses/investigations-structure-porous-media/docview/304208667/se-2?accountid=27575 (accessed on 24 September 2025).
7. Straley, C.; Rossini, D.; Vinegar, H.; Tutunjian, P.; Morriss, C. Core analysis by low field NMR, paper SCA-9404. In *SCA International Symposium Proceedings*; SCA: Stavanger, Norway, 1994. Available online: https://www.ux.uis.no/ s-skj/ipt/Proceedings/SCA.1987-2004/1-SCA1994-04.pdf (accessed on 23 September 2025).
8. Crowe, M.; Jasek, D.; Van Dalen, S.; LaTorraca, G.; Dunn, K.; Donovan, M. Measuring residual oil saturation in west Texas using NMR. In *SPWLA Annual Logging Symposium*; SPWLA: Houston, TX, USA, 1997.
9. Clerke, E.E.; Coates, G.R.; Hartman, D.E.; Horkowitz, J.P.; Vinegar, H.J. Residual oil saturation measurements in carbonates with pulsed NMR logs. *Log Anal.* **1997**, *38*. Available online: https://onepetro.org/petrophysics/article/170917/Residual-Oil-Saturation-Measurements-In-Carbonates (accessed on 1 February 2026).
10. Richardson, J.; Wyman, R.; Jorden, J.; Mitchell, F. Methods for determining residual oil with pulsed neutron capture logs. *J. Pet. Technol.* **1973**, *25*, 593–606. [CrossRef]
11. Coates, G.R.; Xiao, L.; Prammer, M.G. *NMR Logging Principles and Applications*; Gulf Publishing Company: Houston, TX, USA, 1999; pp. 85–87.
12. Yang, P.; Guo, H.; Yang, D. Determination of residual oil distribution during waterflooding in tight oil formations with NMR relaxometry measurements. *Energy Fuels* **2013**, *27*, 5750–5756. [CrossRef]
13. Simpson, G.A.; Fishman, N.S.; Hari-Roy, S. New nuclear magnetic resonance log T2 cut-off interpret parameters for the unconventional tight oil of the bakken petroleum system using 2-D NMR core laboratory measurements on native state and post-cleaned core samples. In *SPWLA Annual Logging Symposium*; SPWLA: Houston, TX, USA, 2018.
14. Sun, B.; Guo, P. The Application of Nuclear Magnetic Resonance 1D T 2 and 2D T 1–T 2 Maps in the Research of Condensate Oil Saturation in Condensate Gas Reservoirs. *Energy Fuels* **2022**, *36*, 7581–7591. [CrossRef]
15. Kuang, L.; Wang, Z.; Feng, C.; Zhao, P.; Mao, R.; Yu, J. Predicting oil saturation of shale-oil reservoirs using nuclear magnetic resonance logs. *Interpretation* **2020**, *8*, SL35–SL43. [CrossRef]
16. Zhang, Y.; Gai, C.; Song, B.; Jiang, J.; Wang, Z. The influence of permeability and heterogeneity on chemical flooding efficiency and remaining oil distribution—Based on NMR displacement imaging. *Sci. Rep.* **2023**, *13*, 14316. [CrossRef] [PubMed]
17. Wu, J.; Li, Q.; Li, Q.; Wang, F.; Cheng, Y.; Yan, C. Design and optimization of bottom-hole temperature–pressure combinations in gas production from gas hydrates via carbon dioxide replacement strategy. *Energies* **2026**, *19*, 3536. [CrossRef]
18. Li, Q.; Wang, F.; Wu, J.; Li, Q.; Zhang, G. Multivariate Coupling Model and Reservoir Characteristics of Enhanced Geothermal Reservoirs. *Energies* **2026**, *19*, 3180. [CrossRef]
19. Ao, F.; Qingchao, L.; Qiang, L.; Jingjuan, W.; Fuling, W.; Chuanliang, Y. Numerical Simulation Investigation of Fracture Propagation Behavior Patterns and Sensitivity Factors of Oil Shale Reservoirs in the Xunyi Region Considering the Influence of Natural Fracture. *Geofluids* **2025**, *2025*, 2762142. [CrossRef]
20. Akin, S.; Kovscek, A. Computed tomography in petroleum engineering research. *Geol. Soc. Lond. Spec. Publ.* **2003**, *215*, 23–38. [CrossRef]
21. Closmann, P.J.; Vinegar, H.J. A technique for measuring steam and water relative permeabilities at residual oil in natural cores: CT scan saturations. *J. Can. Pet. Technol.* **1993**, *32*. [CrossRef]
22. Sedgwick, G.; Miles-Dixon, E. Application Of XRay Imaging Techniques To Oil Sands Experiments. *J. Can. Pet. Technol.* **1988**, *27*. [CrossRef]
23. Akin, S.; Demiral, B. Application of Computerized Tomography to the Determination of Three Phase Relative Permeabilities. 1997. Available online: https://users.metu.edu.tr/serhat/publications/122akin.pdf (accessed on 2 March 2026).
24. Vinegar, H.J.; Wellington, S.L. Tomographic imaging of three-phase flow experiments. *Rev. Sci. Instrum.* **1987**, *58*, 96–107. [CrossRef]
25. Alvestad, J.; Gilje, E.; Hove, A.O.; Langeland, O.; Maldal, T.; Schilling, B.E. Coreflood experiments with surfactant systems for IOR: Computer tomography studies and numerical modelling. *J. Pet. Sci. Eng.* **1992**, *7*, 155–171. [CrossRef]
26. Nagata, R.; Dos Reis, P.J.; Appoloni, C.R. Multi-scale approach to assess total porosity and pore size in four different kinds of carbonate rocks. *Micron* **2023**, *164*, 103385. [CrossRef] [PubMed]
27. Alanazi, A.; Baban, A.; Ali, M.; Keshavarz, A.; Iglauer, S.; Hoteit, H. Residual trapping of CO_2, N_2, and a CO_2-N_2 mixture in Indiana limestone using robust NMR coreflooding: Implications for CO_2 geological storage. *Fuel* **2023**, *353*, 129221. [CrossRef]
28. Manche, C.; Kaczmarek, S.E. PS Evaluation of Mercury Intrusion and Capillary Pressure Results: Development of a New Methodological Approach for Analyzing Carbonates. In Proceedings of the AAPG Annual Convention and Exhibition, Calgary, AB, Canada, 19–22 June 2016.
29. Maas, J.; Springer, N.; Hebing, A.; Berg, S. Displacement Stability Revisited-A New Criterion for the Onset of Viscous Fingering. In Proceedings of the International Symposium of the Society of Core Analysts, Austin, TX, USA, 19–23 September 2022.

30. Maas, J.G.; Springer, N.; Hebing, A.; Snippe, J.; Berg, S. Viscous fingering in CCS-A general criterion for viscous fingering in porous media. *Int. J. Greenh. Gas Control* **2024**, *132*, 104074. [CrossRef]
31. Wang, S.; Tokunaga, T.K. Capillary pressure–saturation relations for supercritical CO_2 and brine in limestone/dolomite sands: Implications for geologic carbon sequestration in carbonate reservoirs. *Environ. Sci. Technol.* **2015**, *49*, 7208–7217. [CrossRef] [PubMed]
32. Christensen, M.; Tanino, Y. Residual oil saturation under mixed-wet conditions: Optimal wettability revisited. In Proceedings of the Proc International Symposium of the Society of Core Analysts, SCA2018–011, Trondheim, Norway, 27–30 August 2018.
33. Mai, A.; Kantzas, A. On the characterization of carbonate reservoirs using low field NMR tools. In Proceedings of the SPE Gas Technology Symposium, Calgary, AB, Canada, 30 April–2 May 2002.
34. Parchekhari, S.; Nakhaee, A.; Kadkhodaie, A.; Khalili, M. Predicting the impact of hydrocarbon saturation on T2 distribution curve of NMR logs–A case study. *J. Pet. Sci. Eng.* **2021**, *204*, 108650. [CrossRef]
35. Hackert, C.L.; Parra, J.O. Simulating NMR magnetization diffusion in a real carbonate pore system. *Petrophysics- SPWLA J. Form. Eval. Reserv. Descr.* **2002**, *43*. Available online: https://onepetro.org/petrophysics/article/171002/Simulating-Nmr-Magnetization-Diffusion-In-A-Real (accessed on 4 February 2026).
36. Kleinberg, R.L. Utility of NMR T2 distributions, connection with capillary pressure, clay effect, and determination of the surface relaxivity parameter ρ2. *Magn. Reson. Imaging* **1996**, *14*, 761–767. [CrossRef] [PubMed]
37. Slijkerman, W.; Hofman, J. Determination of surface relaxivity from NMR diffusion measurements. *Magn. Reson. Imaging* **1998**, *16*, 541–544. [CrossRef] [PubMed]
38. Bendel, P. Spin-echo attenuation by diffusion in nonuniform field gradients. *J. Magn. Reson. (1969)* **1990**, *86*, 509–515. [CrossRef]
39. Fleury, M.; Deflandre, F. Quantitative evaluation of porous media wettability using NMR relaxometry. *Magn. Reson. Imaging* **2003**, *21*, 385–387. [CrossRef] [PubMed]
40. Chen, S.; Ostroff, G.; Georgi, D.T. *Improving Estimation of NMR log T2cutoff Value with Core NMR and Capillary Pressure Measurements*; *SCA*-9822; Western Atlas Logging Service: Houston, TX, USA, 1998; pp. 1–12. Available online: https://www.jgmaas.com/SCA/1998/SCA1998-22.pdf (accessed on 23 September 2025).
41. Dillinger, A.; Esteban, L. Experimental evaluation of reservoir quality in Mesozoic formations of the Perth Basin (Western Australia) by using a laboratory low field nuclear magnetic resonance. *Mar. Pet. Geol.* **2014**, *57*, 455–469. [CrossRef]
42. Marschall, D.; Gardner, J.; Mardon, D.; Coates, G. Method for correlating NMR relaxometry and mercury injection data. In *1995 SCA Conference, Paper*; Society of Core Analysts (SCA); Dublin, CA, USA, 1995. Available online: https://www.jgmaas.com/SCA/1995/SCA1995-11.pdf?utm_source=chatgpt.com (accessed on 24 September 2025).
43. Andersson, L.; Herring, A.; Schlüter, S.; Wildenschild, D. Defining a novel pore-body to pore-throat "Morphological Aspect Ratio" that scales with residual non-wetting phase capillary trapping in porous media. *Adv. Water Resour.* **2018**, *122*, 251–262. [CrossRef]
44. Westphal, H.; Surholt, I.; Kiesl, C.; Thern, H.F.; Kruspe, T. NMR measurements in carbonate rocks: Problems and an approach to a solution. *Pure Appl. Geophys.* **2005**, *162*, 549–570. [CrossRef]
45. Minh, C.C.; Jain, V.; Griffiths, R.; Maggs, D. NMR T2 fluids substitution. In *SPWLA Annual Logging Symposium*; SPWLA: Houston, TX, USA, 2016.
46. Morriss, C.; Rossini, D.; Straley, C.; Tutunjian, P.; Vinegar, H. Core analysis by low-field NMR. *Log Anal.* **1997**, *38*, 84–93. Available online: https://www.jgmaas.com/SCA/1994/SCA1994-04.pdf?utm_source=chatgpt.com (accessed on 23 September 2025).

Disclaimer/Publisher's Note: The statements, opinions and data contained in all publications are solely those of the individual author(s) and contributor(s) and not of MDPI and/or the editor(s). MDPI and/or the editor(s) disclaim responsibility for any injury to people or property resulting from any ideas, methods, instructions or products referred to in the content.